Electroencephalography (EEG)
Recording the brain electric activity

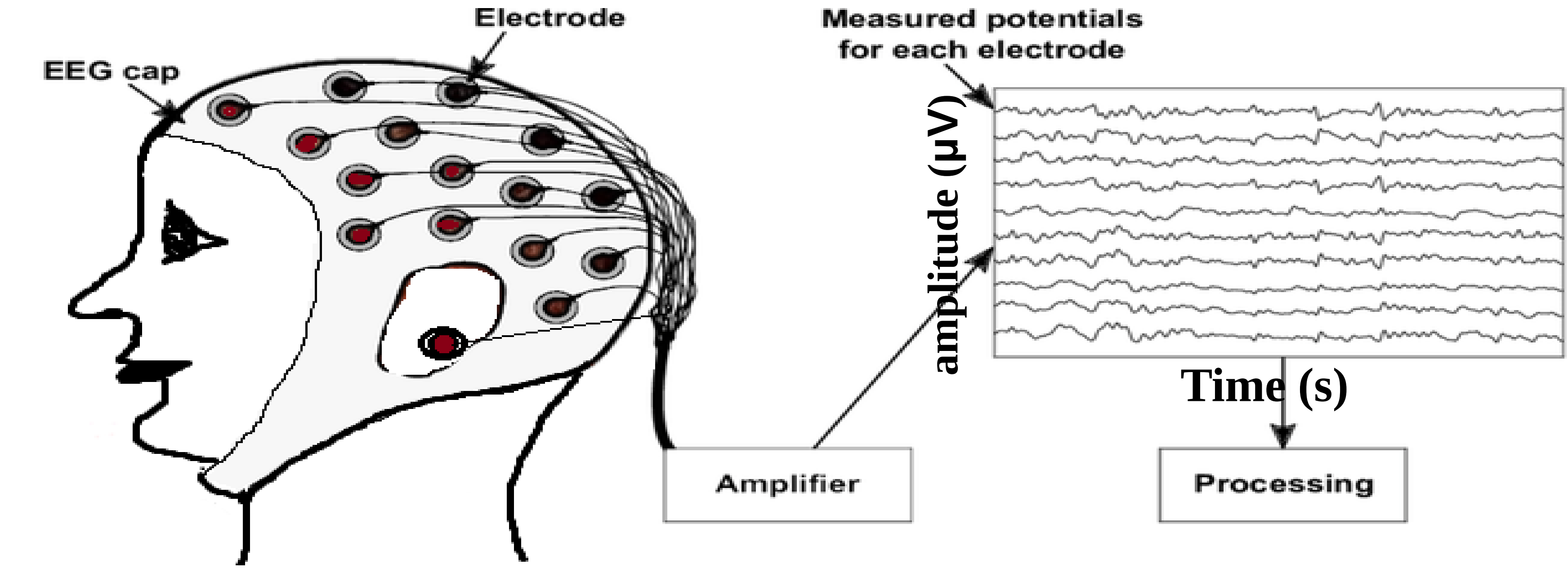

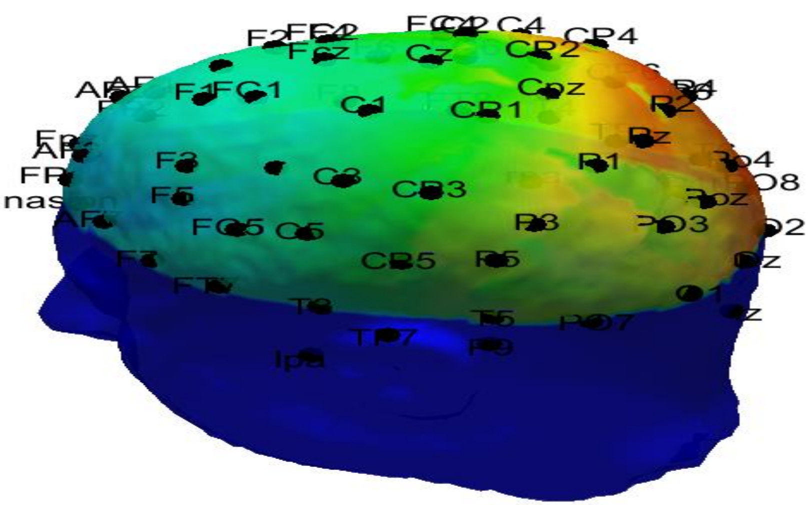

EEG amplitude color-map at an instant

EEG Inverse problem (neural source localization)

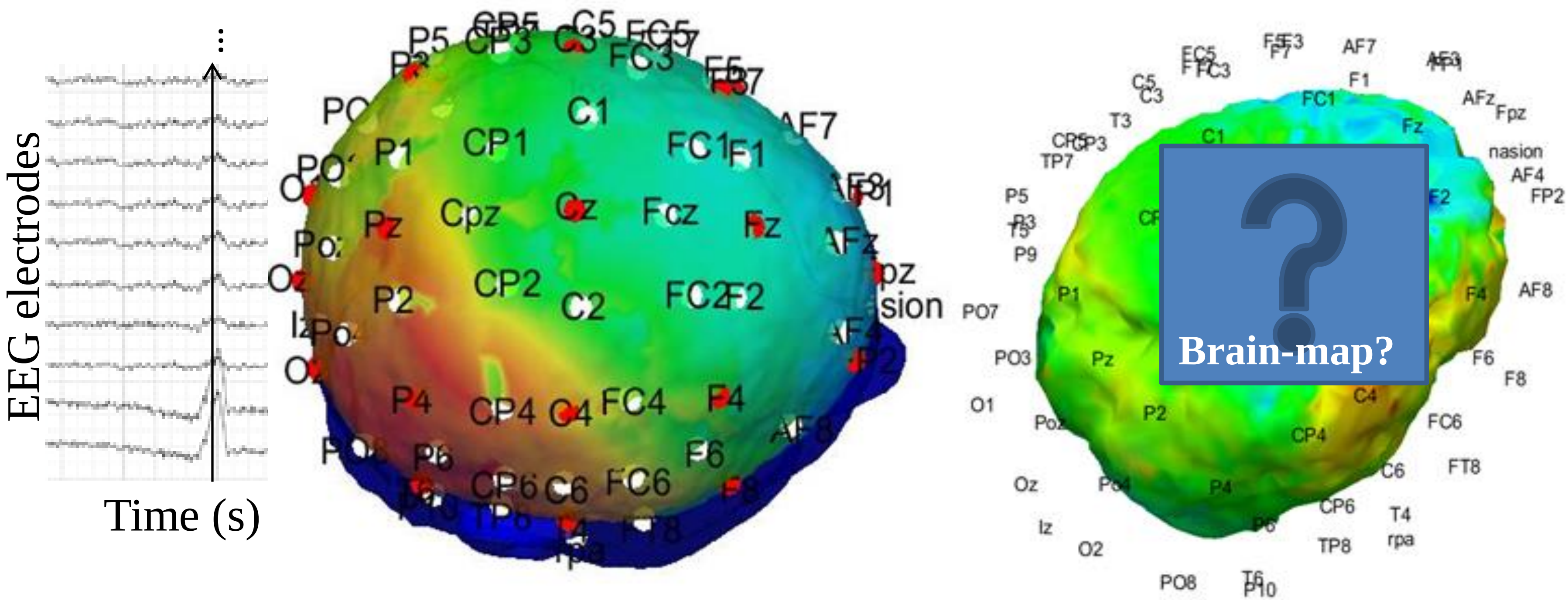

Forward problem (EEG)

1. Neural source localization (inverse problem) is to estimate the cortical neural source signals and brain-map from scalp electric signals (EEG) at each instant during the time.
2. Source localization needs forward problem, i.e. to first estimate how cortical source activity transfers to the scalp.
3. Forward problem estimation is based on an appropriate model for neural source and solving the voltage-current equations in the head volume.

Source localization steps

EEG Neural source model

- The generators of EEG (pyramidal neurons located in gray matter)
- Neural source model : current dipole
- dipole voltage-current equation (Poisson's differential equation)

Head forward problem

Forward problem purpose: How does cortical source activity transfer to scalp?

- Head model definition (MRI acquisition)
- MRI segmentation (scalp, skull, brain segments)
- Mesh generation (scalp, skull, brain surface triangulated mesh)
- Electrode registration on scalp mesh
- Forward problem: Solving Poisson's differential equation (voltage-current equation for head)
- Output of forward problem (solving Poisson's voltage-current equation for head geometry): for each neuronal current source location, source current to each electrode (sensor) voltage is a coefficient called Lead-field or transfer coefficient.
- Lead-field: the feature for each dipole location on gray matter
- Lead-field coefficient: a function of dipole location, head geometry and conductivity.

Inverse problem

- Estimating amplitude of current sources for each cortex location from EEG and inverse algorithms using Lead-field matrix (forward algorithm)

The generators of EEG

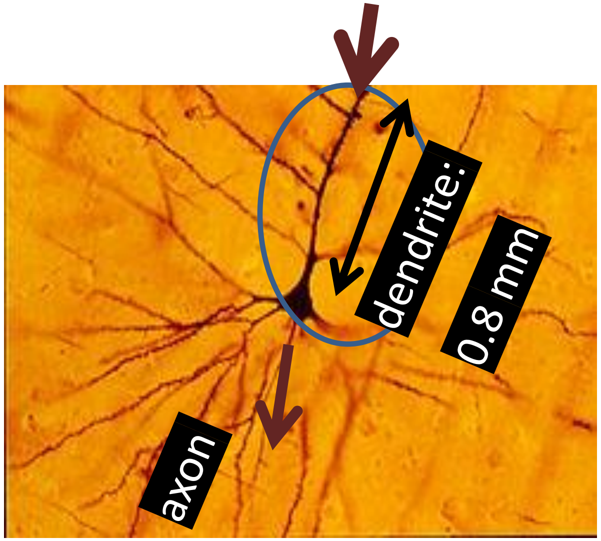

pyramidal neurons visualized by light microscopy technique

Neurotransmitters (in apical dendrite synapses) diffuse positive ions in to neuron

- Dendrite: generators of extracellular potential fields (0.1-10mv)
- Axons: action potential (70-110 mv)
- Pyramidal neurons located in Neocortex (outer layer of cerebral cortex), 2-4mm width (depth)
- Neocortex: 6 layers numbering from outer layer to depth (0.3-0.6 mm width of each layer)
- Layers 3 and 5 are the probable locations for 10-14 billion pyramidal neurons (depth: 0.9-1.8 mm)

Neural source model (current dipole)

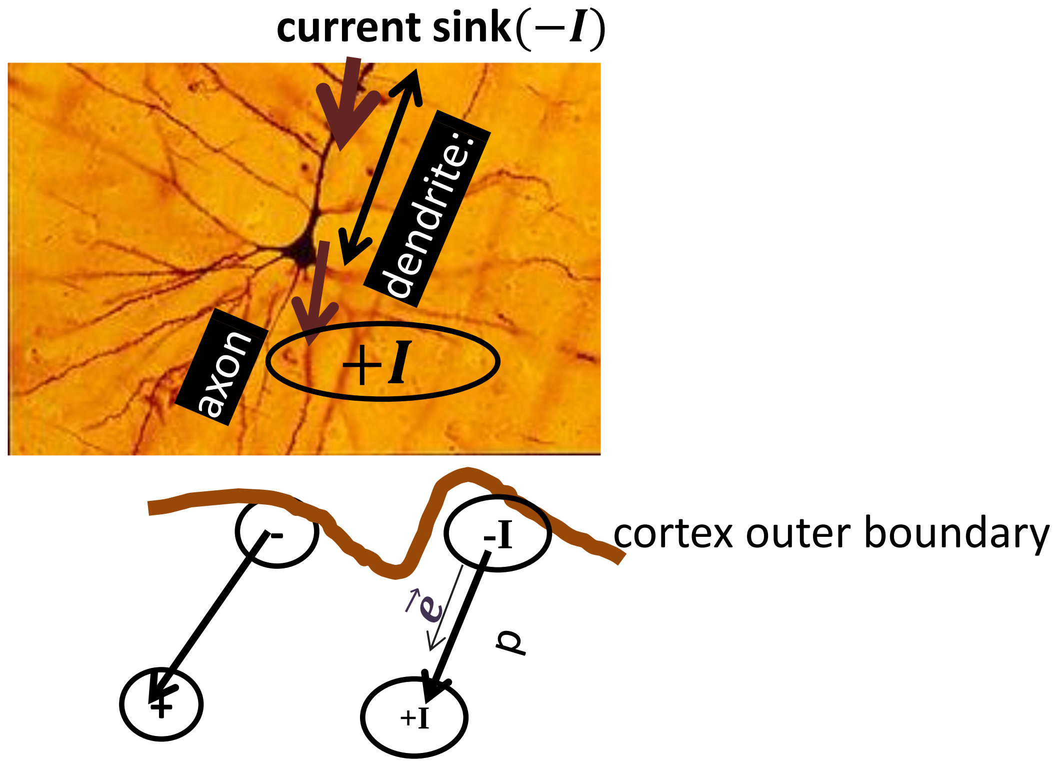

Dipole momentum definition at one point between two monopoles (sink and source)

$$\vec{\boldsymbol{d}} = I.p\ .\ \vec{\boldsymbol{e}} = I.p\ .\vec{\boldsymbol{e}}$$

P: distance between two monopoles (m) usually considered unit (1)

I: current density $({}^{A}/_{m^2})$

$\vec{\boldsymbol{e}}$: vector from sink to source (two monopoles), this vector is normal to surface on outer layer of gray matter (cerebral cortex)

dipole voltage-current equation

$$\boldsymbol{J} = \boldsymbol{J}^{\boldsymbol{p}} + \boldsymbol{\sigma E}$$

$\boldsymbol{J}$ $(^{\boldsymbol{A}}/_{\boldsymbol{m^2}})$**:** total current density

$\boldsymbol{\sigma}$: conductivity

$\boldsymbol{J}^{\boldsymbol{p}}$: primary current density(in or near to cell)

$\boldsymbol{\sigma E}$**:** secondary (volume) current

A small volume around neuron has no net current.

$$\boldsymbol{J} = \boldsymbol{\nabla} \times \boldsymbol{B} \rightarrow \ \boldsymbol{\nabla}.\boldsymbol{J} = \boldsymbol{\nabla}.(\boldsymbol{\nabla} \times \boldsymbol{B}) = \boldsymbol{0}$$

$$\boldsymbol{J} = \boldsymbol{J}^{\boldsymbol{p}} + \boldsymbol{\sigma E} = \boldsymbol{J}^{\boldsymbol{p}} - \boldsymbol{\sigma \nabla V}$$

$\boldsymbol{\nabla}.(\boldsymbol{\sigma \nabla V}) = \boldsymbol{\nabla}.\boldsymbol{J}^{\boldsymbol{p}}$: **This is called the Poisson's differential equation**

So $\boldsymbol{J}^{\boldsymbol{p}}$**, primary current density, is the EEG source.**

$$\boldsymbol{\nabla}.\boldsymbol{J}^{\boldsymbol{p}} = -\boldsymbol{I\delta}(\boldsymbol{r} - \boldsymbol{r}_{\boldsymbol{sink}}) + \boldsymbol{I\delta}(\boldsymbol{r} - \boldsymbol{r}_{\boldsymbol{source}})$$

Solving Poisson's equation = primary current density estimation

Head model definition (MRI)

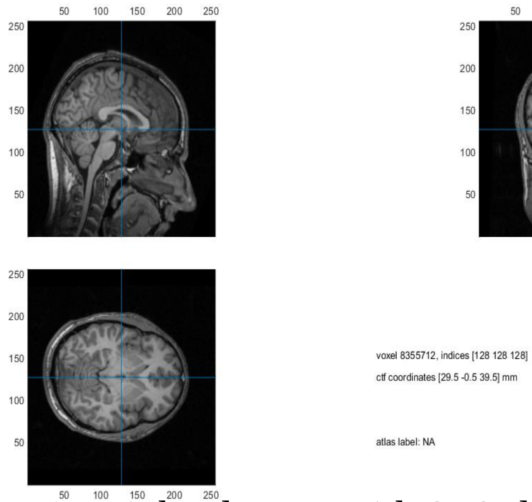

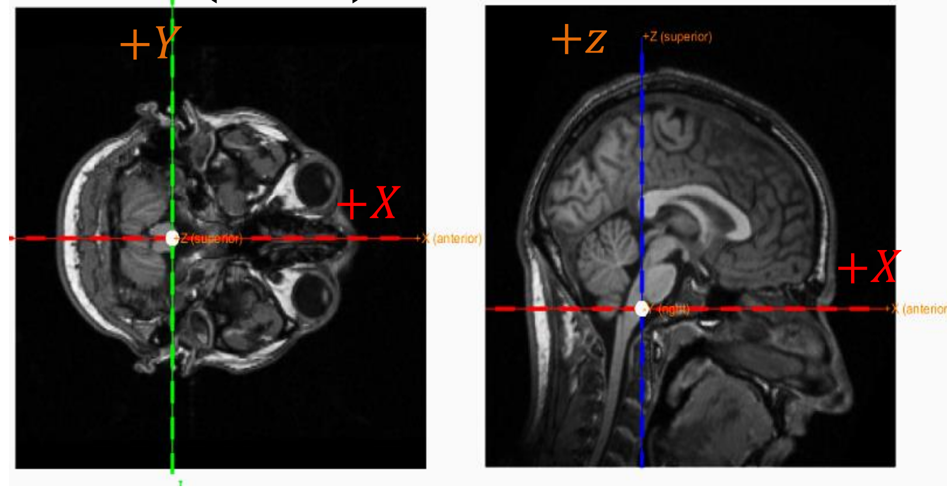

Left: T1 weighted MRI With 256 slices (plates) of each 256*256 voxels (cubes)

Right: MRI coordinate system, Define +X+Y+Z MRI coordsys corresponding anatomical directions, (A)nterior (nose)/(P)osterior (inion), (S)uperior (vertex)/(I)nferior, (R)ight (ear)/(L)eft. The coordsys is ‘ALS’ and center of coordsys is inter auricular (between ears)

MRI has a transformation matrix for transforming each voxel (cube) location from voxel space (i, j, k) to 3d (x, y, z) real location in MRI coordsys. Each voxel is discretized by it’s location and intensity (gray level)

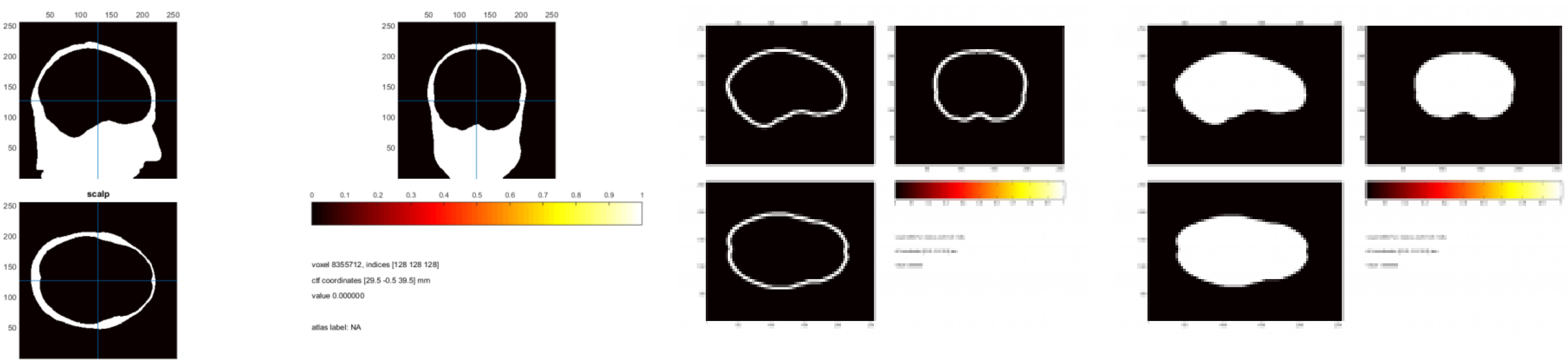

Segmented MRI (scalp, skull, brain segments). Method: Allocating different gray levels to different tissues (scalp, skull, gray matter) based on tissue probability maps form MRI atlases besides tissue morphology, good tools to segment head tissues [7].

Mesh generation

Gray matter mesh | Skull mesh | Scalp mesh and EEG electrodes

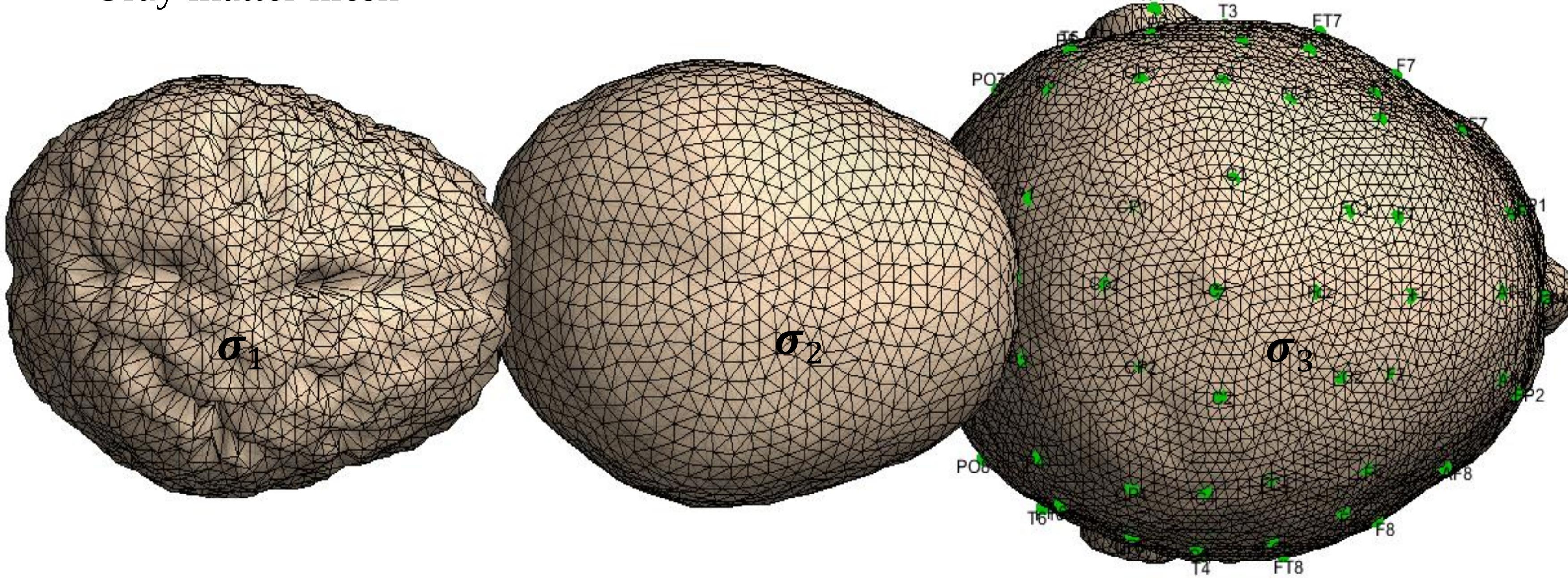

Surface triangulated meshes (brain, skull, scalp interfaces (boundaries)) [8] acquired from segmented MRI and their conductivities ($\boldsymbol{\sigma}_1, \boldsymbol{\sigma}_2, \boldsymbol{\sigma}_3$),

$$\boldsymbol{\sigma}_1 \approx \boldsymbol{\sigma}_3 = a\,\boldsymbol{\sigma}_2$$

$\boldsymbol{\sigma}_1 \approx \boldsymbol{\sigma}_3$=0.33, $a = 15 - 80$, most reported $a = 25$. [2]

Conductivities are acquired with different techniques [2] such as electric impedance tomography (EIT, an imaging technique which applies source-sink currents to paired scalp electrodes and images scalp potentials using forward problem and an other concept based reciprocity in electronic circuits).

Electrode registration on scalp mesh

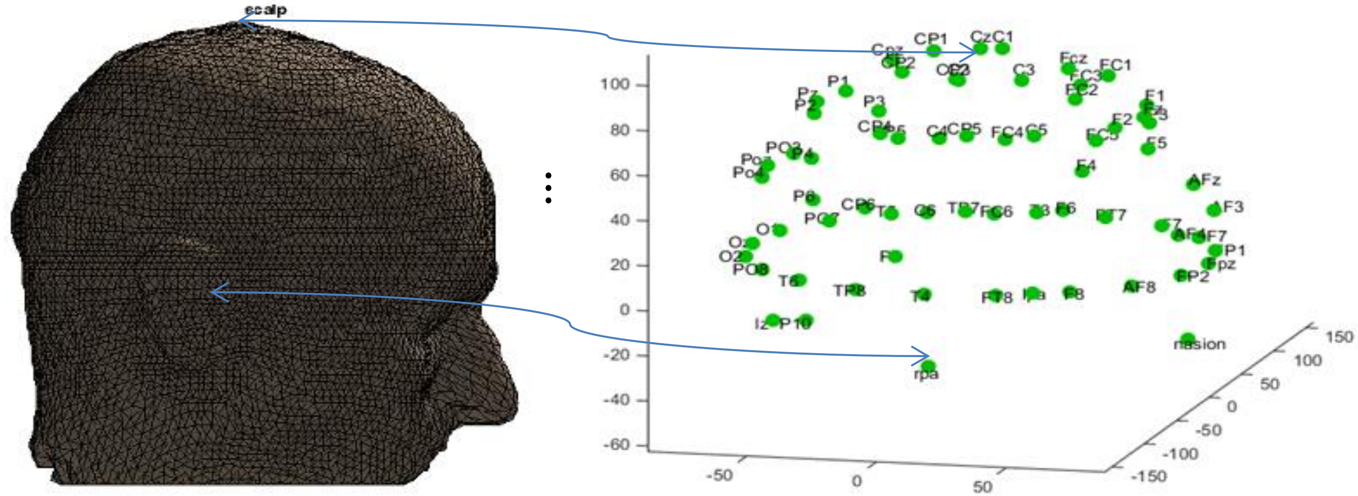

Scalp mesh and Primary electrodes defined on a sphere according to 10-10 standard

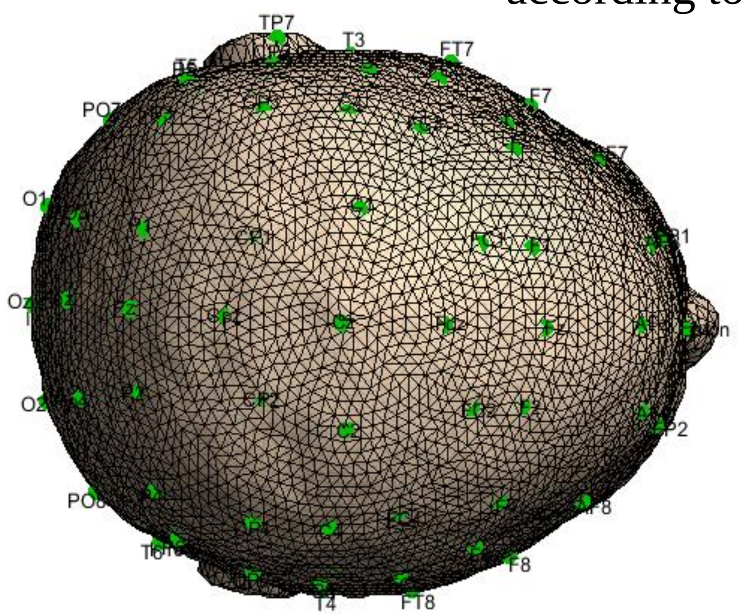

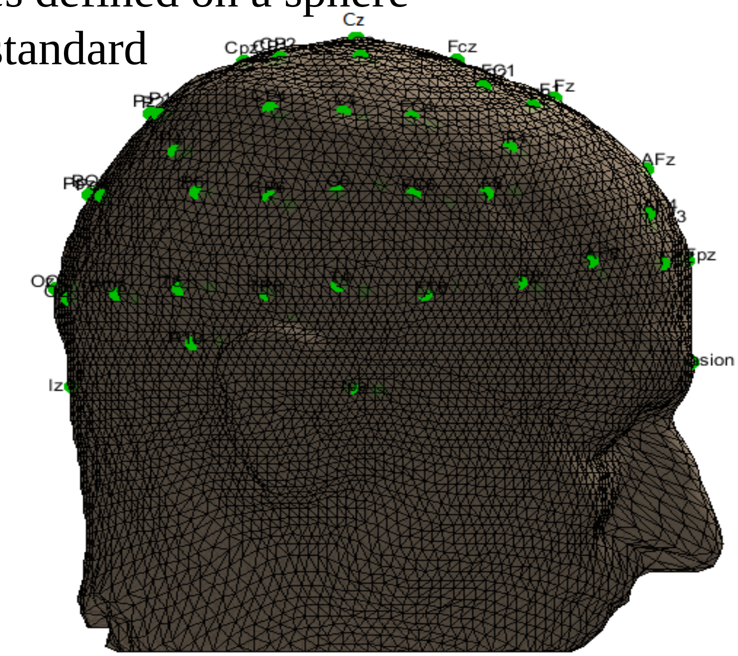

Final electrode registration, Methods: iterative closest point (ICP) [5][6] and warping, registration error as RMS distance of electrodes to scalp mesh nodes : 0.3mm

piecewise homogeneous medium

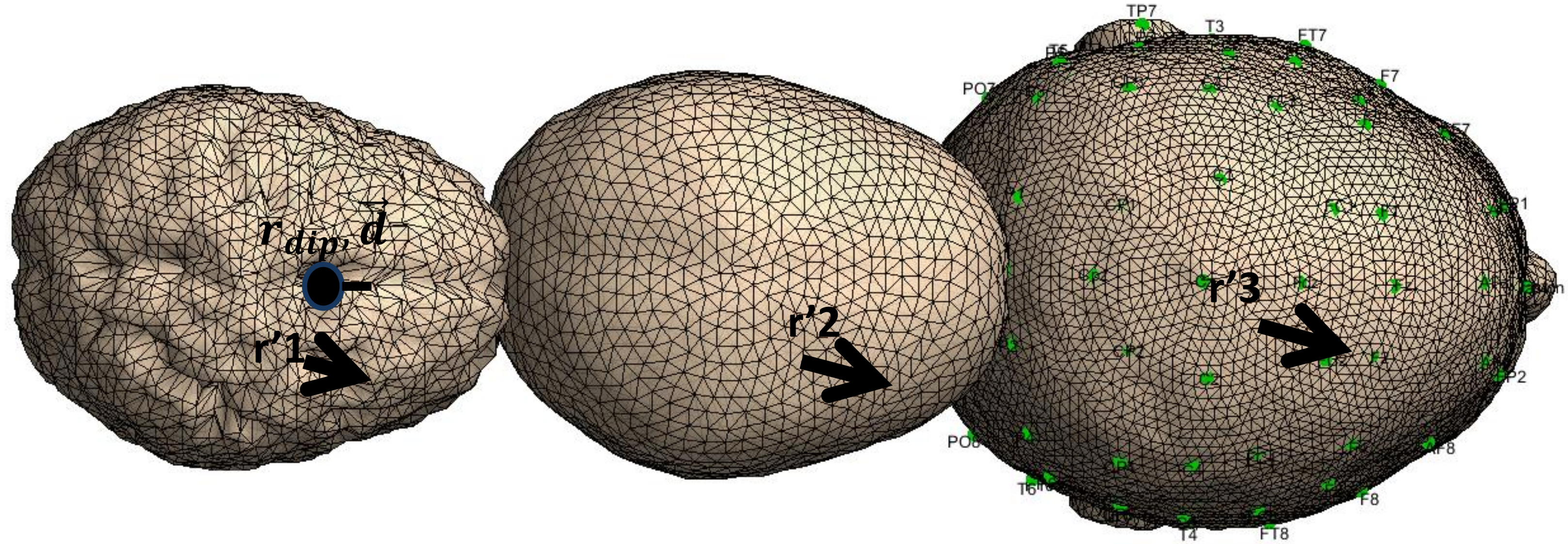

r': any point on triangles ($r' = r'_1, r'_2, r'_3$)

dipole general directions at one location (1,0,0) (0,1,0) (0,0,1)

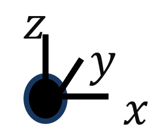

dipole momentum vector: $\vec{\boldsymbol{d}} = \vec{\boldsymbol{e}}_{\boldsymbol{d}(\mathbf{3}*\mathbf{1})} * \boldsymbol{d}$

$\boldsymbol{d}$ dipole magnitude (dipole current density $\boldsymbol{J}$ $({}^{A}/_{m^2})$)

$\vec{\boldsymbol{e}}_{\boldsymbol{d}(\mathbf{3}*\mathbf{1})}$: dipole normalized vector direction

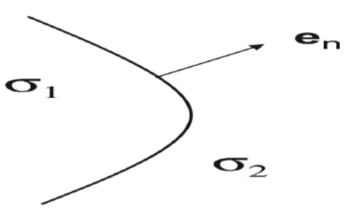

Two boundary conditions at gray/skull, skull/scalp, scalp/air interfaces (boundaries)

$\boldsymbol{J}_{\mathbf{1}}.\boldsymbol{e}_{\boldsymbol{n}} = \boldsymbol{J}_{\mathbf{2}}.\boldsymbol{e}_{\boldsymbol{n}},$ current density is continuous in boundaries

$(\boldsymbol{\sigma}_{\mathbf{1}}\nabla\boldsymbol{V}_{\mathbf{1}}).\boldsymbol{e}_{\boldsymbol{n}} = (\boldsymbol{\sigma}_{\mathbf{2}}\nabla\boldsymbol{V}_{\mathbf{2}}).\boldsymbol{e}_{\boldsymbol{n}}$, σ_1 and σ_2 inner and outer interface conductivity

at the surface of scalp:$\boldsymbol{J}_{\mathbf{1}}.\boldsymbol{e}_{\boldsymbol{n}} = \mathbf{0}, (\boldsymbol{\sigma}_{\mathbf{1}}\nabla\boldsymbol{V}_{\mathbf{1}}).\boldsymbol{e}_{\boldsymbol{n}} = \mathbf{0}$

The other boundary condition in interfaces (except air): $\boldsymbol{V}_{\mathbf{1}} = \boldsymbol{V}_{\mathbf{2}}$

Solving Poisson's equation (for a dipole in infinite homogeneous medium)

$$V_0\left(\boldsymbol{r}, \boldsymbol{r}_{dip}, \vec{\boldsymbol{d}}\right) = \frac{\vec{\boldsymbol{d}}.\left(\boldsymbol{r} - \boldsymbol{r}_{dip}\right)}{4\pi\sigma_0\left\|\boldsymbol{r} - \boldsymbol{r}_{dip}\right\|^3}$$

V_0: potential at any point in infinite homogeneous medium

r: any point in space

$\boldsymbol{r}_{dip}$: dipole location

$\vec{\boldsymbol{d}}$: dipole moment

σ_0: medium conductivity (s/m)

Solving Poisson's equation for a dipole in piecewise homogeneous medium (head)
Boundary element method (BEM)

$$\boldsymbol{V}(\boldsymbol{r}) = \frac{2\sigma_0}{\sigma_r^- + \sigma_r^+} V_o\ (\boldsymbol{r}) + \sum_{triangles\ on\ boundaries} \text{function (voltage, geometry, conductivity on each triangle)}$$

${\sigma_r}^{\pm}$: conductivity (s/m) of outer (+)/inner(-) medium at location $\boldsymbol{r}$
Note: $\boldsymbol{r}$ belongs to one triangle

$$\boldsymbol{V}(r) = \frac{2\sigma_0}{\sigma_r^- + \sigma_r^+}V_o(\boldsymbol{r}) + \frac{1}{2\pi}\sum_{k=1}^{R=3}\frac{\sigma_k^- - \sigma_k^+}{\sigma_r^- + \sigma_r^+}\sum_{j=1}^{N_{s_k}}\sum_{i=1}^{N_{s_k}} V_i^k \int_{\Delta_{s_{k,j}}} h_i(\boldsymbol{r})\frac{\boldsymbol{r}' - \boldsymbol{r}}{\|\boldsymbol{r}' - \boldsymbol{r}\|^3}\,dS_k$$

$\sigma_k{}^{\pm}$: conductivity (s/m) on kth outer (+)/inner(-) interface (boundary) gray/skull interface, skull/scalp interface, scalp/air interface

σ_0*: dipole medium (*gray matter) conductivity (equal $\sigma_1{}^{-}$)

Surface integral is calculated along normal vector ($\vec{n}$) on each of N_{s_k} triangles (geometry dependent) with unknown voltages V_i^k.

V_i^k: all unknown potentials on N_{s_k} triangles on each boundary, hence the above equation is not solvable.

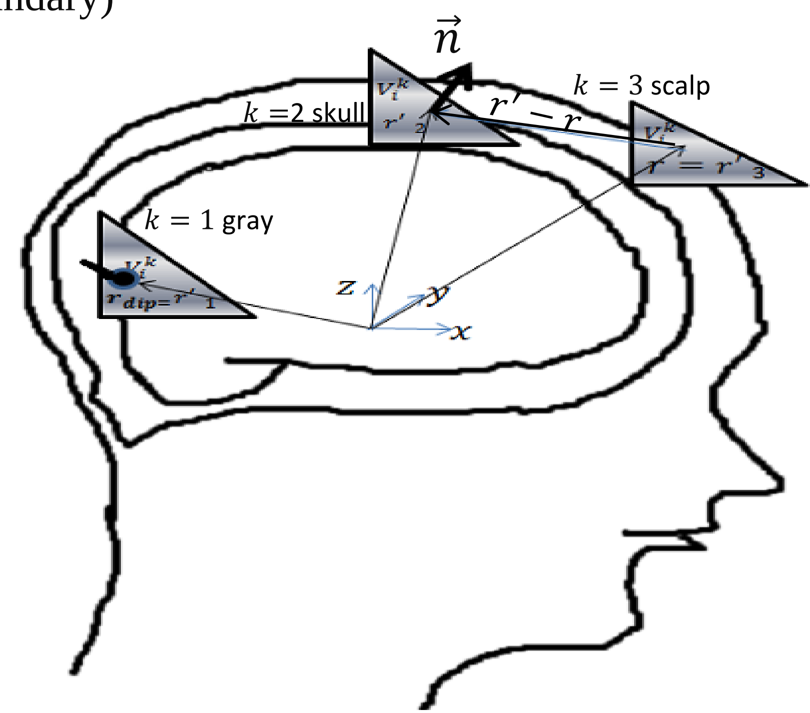

$h_i(\boldsymbol{r})$ basis function is defined to simplify the equation by lowering the unknowns and making equation solvable.

$h_i(\boldsymbol{r})$: basis function of $\boldsymbol{r}$ decreasing with increasing distance to $\boldsymbol{r}$, a simple definition $h_i(r) = \begin{cases} 1 & \boldsymbol{r} \in \Delta_i \\ 0 & \boldsymbol{r} \notin \Delta_i \end{cases}$, Δ_i is the i-th planar triangle on the tessellated surface.

$\boldsymbol{r}'$: any point on triangles of surface meshes of scalp, skull, gray matter ($\boldsymbol{r}' = \boldsymbol{r}'_1, \boldsymbol{r}'_2, \boldsymbol{r}'_3$),

$\boldsymbol{r}$: any point on surface meshes of scalp, skull, gray matter (the purpose location is on scalp, $\boldsymbol{r}'_3$),

R: number of interfaces (boundaries) (3 boundaries), N_{s_k}: number of triangles on k-th boundary,($k = 1, 2, 3$)

A $\boldsymbol{conclusion}$: $\boldsymbol{V(r) = function(conductivity, geometry, \vec{d})}$

It is proved: $\boldsymbol{V} \alpha\, \boldsymbol{V_0}\, \alpha\, \vec{\boldsymbol{d}}$; $V_0\left(\boldsymbol{r}, \boldsymbol{r}_{dip}, \vec{\boldsymbol{d}}\right) = \frac{\vec{\boldsymbol{d}}.(\boldsymbol{r}-\boldsymbol{r}_{\boldsymbol{dip}})}{4\pi\sigma_0 \left\|\boldsymbol{r}-\boldsymbol{r}_{\boldsymbol{dip}}\right\|^3}$

$$\boldsymbol{V(r)} = \mathbf{function(conductivity, geometry)} * \vec{\boldsymbol{d}} = \mathbf{Lead - field} * \vec{\boldsymbol{d}},$$

leadfield is a constant parameter for each dipole location

for $\boldsymbol{M}$ electrodes and $\boldsymbol{n_d}$ dipoles at time $\boldsymbol{t_i}$ we have:

momentum for dipole location 1
At time t_i

$$\begin{bmatrix} L_1^{1,x} & L_1^{1,y} & L_1^{1,z} & \dots & L_1^{\boldsymbol{n_d},x} & L_1^{\boldsymbol{n_d},y} & L_1^{\boldsymbol{n_d},z} \\ L_2^{1,x} & L_2^{1,y} & L_2^{1,z} & \dots & L_2^{\boldsymbol{n_d},x} & L_2^{\boldsymbol{n_d},y} & L_2^{\boldsymbol{n_d},z} \\ \dots & \dots & \dots & \dots & \dots & \dots & \dots \\ L_M^{1,x} & L_M^{1,y} & L_M^{1,z} & \dots & L_M^{\boldsymbol{n_d},x} & L_M^{\boldsymbol{n_d},y} & L_M^{\boldsymbol{n_d},z} \end{bmatrix} \begin{bmatrix} d^{1,x,t_i} \\ d^{1,y,t_i} \\ d^{1,z,t_i} \\ \dots \\ d^{\boldsymbol{n_d},x,t_i} \\ d^{\boldsymbol{n_d},y,t_i} \\ d^{\boldsymbol{n_d},z,t_i} \end{bmatrix} = \begin{bmatrix} V_1 \\ V_2 \\ \dots \\ V_M \end{bmatrix}$$

Lead-field for dipole location 1
with 3 general Cartesian directions (x, y, z)

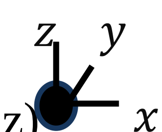

Scalp potentials at M electrodes
from n_d dipoles at time t_i

momentum for dipole location 1
At time t_i

Dipolar sources
+
Head model
(describing conductivity and geometry)

Lead-fields

$$\begin{bmatrix} L_1^{1,x} & L_1^{1,y} & L_1^{1,z} & \dots & L_1^{n_d,x} & L_1^{n_d,y} & L_1^{n_d,z} \\ L_2^{1,x} & L_2^{1,y} & L_2^{1,z} & \dots & L_2^{n_d,x} & L_2^{n_d,y} & L_2^{n_d,z} \\ \dots & \dots & \dots & \dots & \dots & \dots & \dots \\ L_M^{1,x} & L_M^{1,y} & L_M^{1,z} & \dots & L_M^{n_d,x} & L_M^{n_d,y} & L_M^{n_d,z} \end{bmatrix} \begin{bmatrix} d^{1,x,t_i} \\ d^{1,y,t_i} \\ d^{1,z,t_i} \\ \dots \\ d^{n_d,x,t_i} \\ d^{n_d,y,t_i} \\ d^{n_d,z,t_i} \end{bmatrix} = \begin{bmatrix} V_1 \\ V_2 \\ \dots \\ V_M \end{bmatrix}$$

Lead-field for dipole location 1

Scalp potentials at M electrodes
from n_d dipoles at time t_i

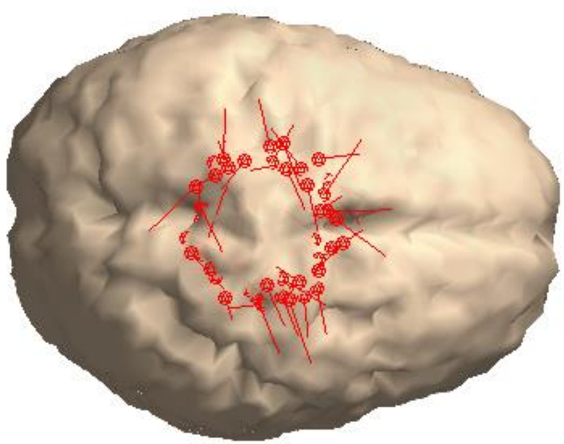

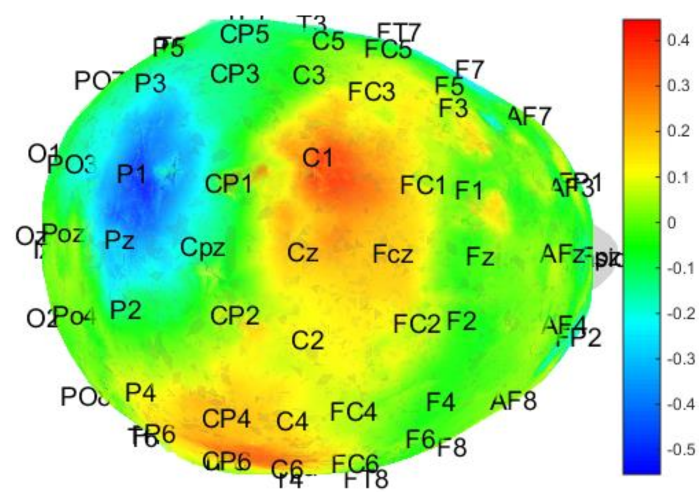

Mapping lead-fields on electrodes for n_d=50
dipolar sources with amplitude=1 and normal directions to gray matter surface mesh

Inverse problem (source estimation)

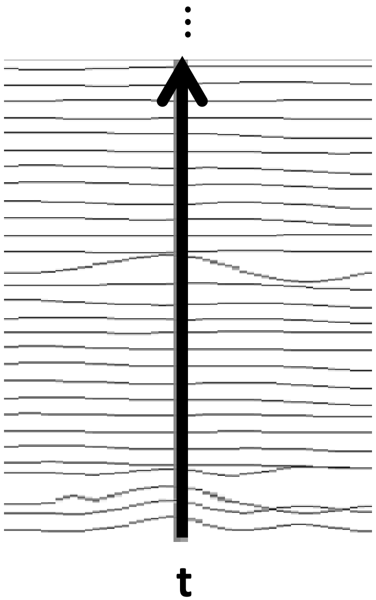

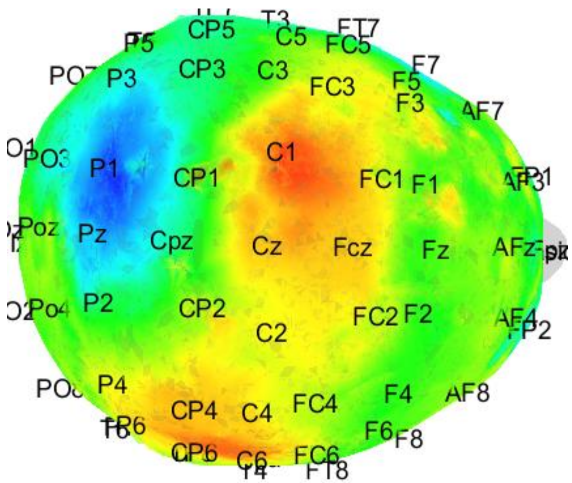

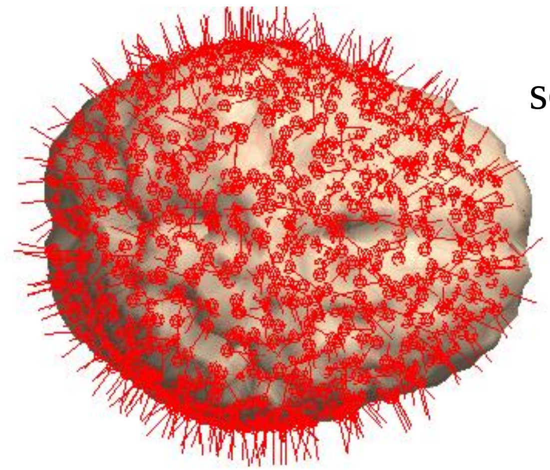

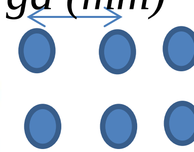

Left: EEG and EEG-map at one time sample (known)

Right: A set of dipole sources (with unknown amplitudes, known lead-fields), predefined and distributed on gray matter. Sources can be distributed on a grid (a set of location points) with a predefined minimum grid distance (*gd (mm)*)

$$\boldsymbol{L_{forward}\vec{d} = EEG}$$

Inverse

$$\boldsymbol{\vec{d} = L_{inverse}{}^{\dagger}\, EEG = (L_{inverse}{}'L_{inverse})^{-1}L_{inverse}{}'\, EEG}$$

$\boldsymbol{L_{forward}}$: Lead-field Matrix with $3 * n_d$ columns corresponding n_d active sources

Each 3 columns of $\boldsymbol{L_{inverse}}$ is Lead-field corresponding each predefined source location

✓ distributed dipole source over large area of brain (since we don't know exact locations of sources), hence $\boldsymbol{L_{inverse}}$ is a large matrix.

Problems with large $\boldsymbol{L_{inverse}}$:

- Any small change in EEG may cause a large change in $\vec{\boldsymbol{d}}$
- Reason: <u>eigenvalues</u> / singular values of $\boldsymbol{L_{inverse}}^{\dagger}$ are largest in the reverse mapping where they were smallest in the forward mapping ($\boldsymbol{L_{forward}}$). High Eigen value causes discontinuous change in $\vec{\boldsymbol{d}}$ with a little change in $\boldsymbol{EEG}$.
- <u>Condition number:</u> $\boldsymbol{K(L'L)} = \|(\boldsymbol{L'L})\| \left\|(\boldsymbol{L'L})^{-1}\right\| = \max(\boldsymbol{eig(L'L)}) / \boldsymbol{min}(\boldsymbol{eig(L'L)}),$
- $\boldsymbol{eig}$: Eigen value $\boldsymbol{L}$=$\boldsymbol{L_{inverse}}$

<u>Higher Condition number increases the probability for discontinuity of source signal estimations.</u>

Solution for achieving low condition number, well-posed (unique best approximate) solver for $\vec{\boldsymbol{d}}$:

$\vec{\boldsymbol{d}} = (\boldsymbol{L'L} + \alpha\, \boldsymbol{I})^{-1}\boldsymbol{L'}\ \boldsymbol{EEG}$, $(\boldsymbol{L'L} + \alpha\, \boldsymbol{I})$ has lower Condition number

I: identity matrix, α: Tikhonov regularization number

$$\boldsymbol{Min}\ \ \boldsymbol{F_\alpha}(\vec{\boldsymbol{d}}) = \left\|\boldsymbol{L}\vec{\boldsymbol{d}} - \boldsymbol{EEG}\ \right\|^2 + \alpha\left\|\vec{\boldsymbol{d}}\right\|^2$$

minimum norm inverse solution

General form for minimum norm inverse solution:

$$\boldsymbol{Min}\ \ \boldsymbol{F_\alpha}(\vec{\boldsymbol{d}}) = \left\|\boldsymbol{L}\vec{\boldsymbol{d}} - \boldsymbol{EEG}\ \right\|^2 + \alpha\left\|\boldsymbol{W}\vec{\boldsymbol{d}}\right\|^2$$

$\boldsymbol{W}$: weight matrix, α: Tikhonov regularization number

different weights ≡ different minimum norm inverse methods.

$\boldsymbol{P}(\alpha) = \left\|\boldsymbol{L}\vec{\boldsymbol{d}}(\alpha) - \boldsymbol{EEG}\ \right\|^2 \left\|\vec{\boldsymbol{d}}(\alpha)\right\|^2$

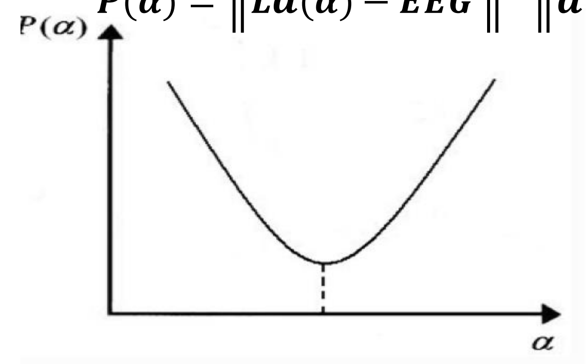

Inverse methods	weight matrix (W)	Output dipole current sources ($\vec{d}$)
MNE (Minimum norm estimate)	**W=I (identity matrix)**	$\vec{d} = (L'L + \alpha\, W'W)^{-1} L'\, EEG$
WMNE (weighted Minimum norm estimate)	**W= B** $\mathbf{B} = \mathbf{diag(norm(columns\ (L)))}$ $\boldsymbol{Diag}(\ldots)$: diagonal matrix with non zero components in diagonal, each component is norm of one column of **L** This compensates for lower gains of different locations by MNE	$\vec{d} = (L'L + \alpha\, W'W)^{-1} L'\, EEG$
LORETA (Low resolution electromagnetic tomography)	**W=ΔB,** Δ: **laplacian operator** $\mathbf{B} = \mathbf{diag(norm(columns\ (L)))}$ Diag(…): diagonal matrix with non zero components in diagonal, each component is norm of one column of L **laplacian of $\mathbf{B_i}$** for each source location: $\frac{1}{d}\left(6B_i - \sum_{i=1}^{p} B_p\right)$, $\forall \mathbf{p}$ under constraint $\left\lVert r_i - r_p \right\rVert = d1$ $d1$: minimum distance between two gridpoints This increases spatial resolution of source localization.	$\vec{d} = (L'L + \alpha\, W'W)^{-1} L'\, EEG$

<table>
<tr><td>LAURA (local autoregressive averages)</td><td>$W_j = (W_m A)'(W_m A)^\wedge I_3$
^: kronecker matrix product (each row-element in first matrix multiplied by all row-elements of other matrix)
$W_m = \mathbf{diag}(\mathbf{mean}(\mathbf{norm}(\mathbf{3}_{\mathbf{columns}}(\mathbf{L}))))$
Diag(…): diagonal matrix with non zero components in diagonal, each component is mean(average) of norm of 3 column of L
A: distance matrix, for hexahedral grid
A_{ii}=26/num nearestneighbours $(\sum_{K=1:\text{num\_nearestneighbours}} d1_{ki}{}^{-3})$
$A_{ki} = d1_{ki}{}^{-3}$, $d1_{ki}$: distance between k-th and i-th grid point
A is defined based on Physiological constraints from forward problem (based poison's equation)
Reason:
$$V_o(r) = \frac{d.(r - r_{dip})}{4\pi\sigma\|r - r_{dip}\|^3} = \frac{\|d\| \cos(\theta)}{4\pi\sigma\|r - r_{dip}\|^2}$$
$J = \vec{d}$ dipole current , $J = \sigma E = \sigma(-\nabla V), \nabla$: gradient
$J\alpha \frac{1}{\|\hat{r}\|^3}$, $\hat{r}=(r - r_{dip})$, <u>in head volume J attenuates with power 3 of distance to source</u></td><td>$\vec{d} = W_j L'(LW_j{}^{-1}L'\alpha I)^{-1}EEG$</td></tr>
<tr><td>EPIFOCUS</td><td>T=L*W L:leadfield matrix,
W= B, B = $\mathbf{diag}(\mathbf{1/norm}(\mathbf{columns}\ (\mathbf{L})))$
Diag(…): diagonal matrix with non zero components in diagonal, each component is 1/norm of one column of L
$$G = \begin{bmatrix} T_1{}^\dagger \\ T_2{}^\dagger \\ \dots \\ T_{np}{}^\dagger \end{bmatrix}, T_i^\dagger: \textit{pseudo inverse of each three columns of } T$$
$T_1{}^\dagger = (T_1{}^T T_1)^{-1} T_1{}^T$
The idea for dividing by norm: reducing the condition number. The idea behind this method is based on subspace reconstructions of a matrix</td><td>$\vec{d}$=G*EEG</td></tr>
</table>

Inverse problem steps
(source estimation and localization steps at one sample time on the EEG)

Source estimation:

$$\vec{d} = (L'L + \alpha W'W)^{-1}L' \, EEG$$

calculating the magnitude (modulus) of each source after estimation of $\vec{d}$, Magnitude $(\vec{d}) = \sqrt[2]{d_x^2 + d_y^2 + d_z^2}$

Source detection (localization):

Comparing magnitudes and selecting sources locations with magnitudes more than a threshold

Distance Error:

$$\vec{a} = location_{detected\ source} - location_{real\ source}, \quad distance = \sqrt[2]{a_x^2 + a_y^2 + a_z^2}$$

1. For each real source location (from intracranial recordings) distance to all detected source locations (from inverse algorithm) is computed and the $minimum\_distance$ (nearest one) is selected.
2. $Average - Distance - Error$ = Average of $minimum\_distance$ for all real sources
3. $Average - Distance\ Error - in\ grid - unit = Average - Distance - Error/gd$

- Lower $Average - Distance - Error$ is an evaluation number for accuracy of an inverse method
- Real sources are often concentrated in a region in source grid with minimum grid distance gd(mm).

1. for each detected source location (from inverse algorithm), distance to all real source locations is computed and the $minimum\_distance$ is selected for each detected source.
2. Percentage of detected sources located with $minimum\_distance$ to real source region in the range [0 1) grid-unit(gd(mm)), [1 2) grid-unit (gd(mm)),… is an other evaluation parameter for accuracy of an inverse method. Higher percent in [0 1) grid-uni shows more accurate source localization.
3. Refer to [9] for comparison of the accuracy of source localization methods and refer to [10] for increasing the accuracy with source connectivity analysis..

Inverse problem (LORETA source localization)

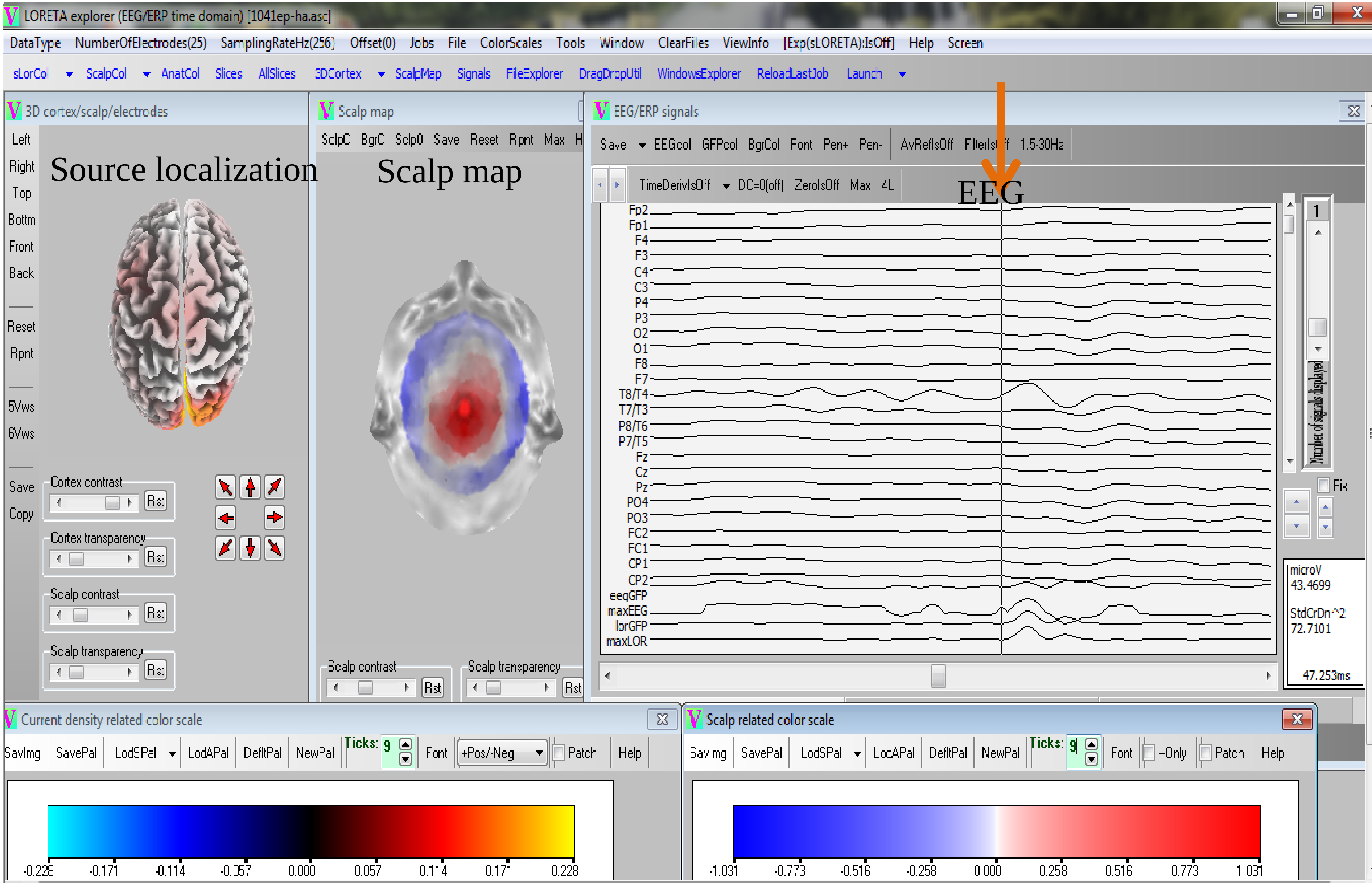

Inverse problem (LORETA source localization)

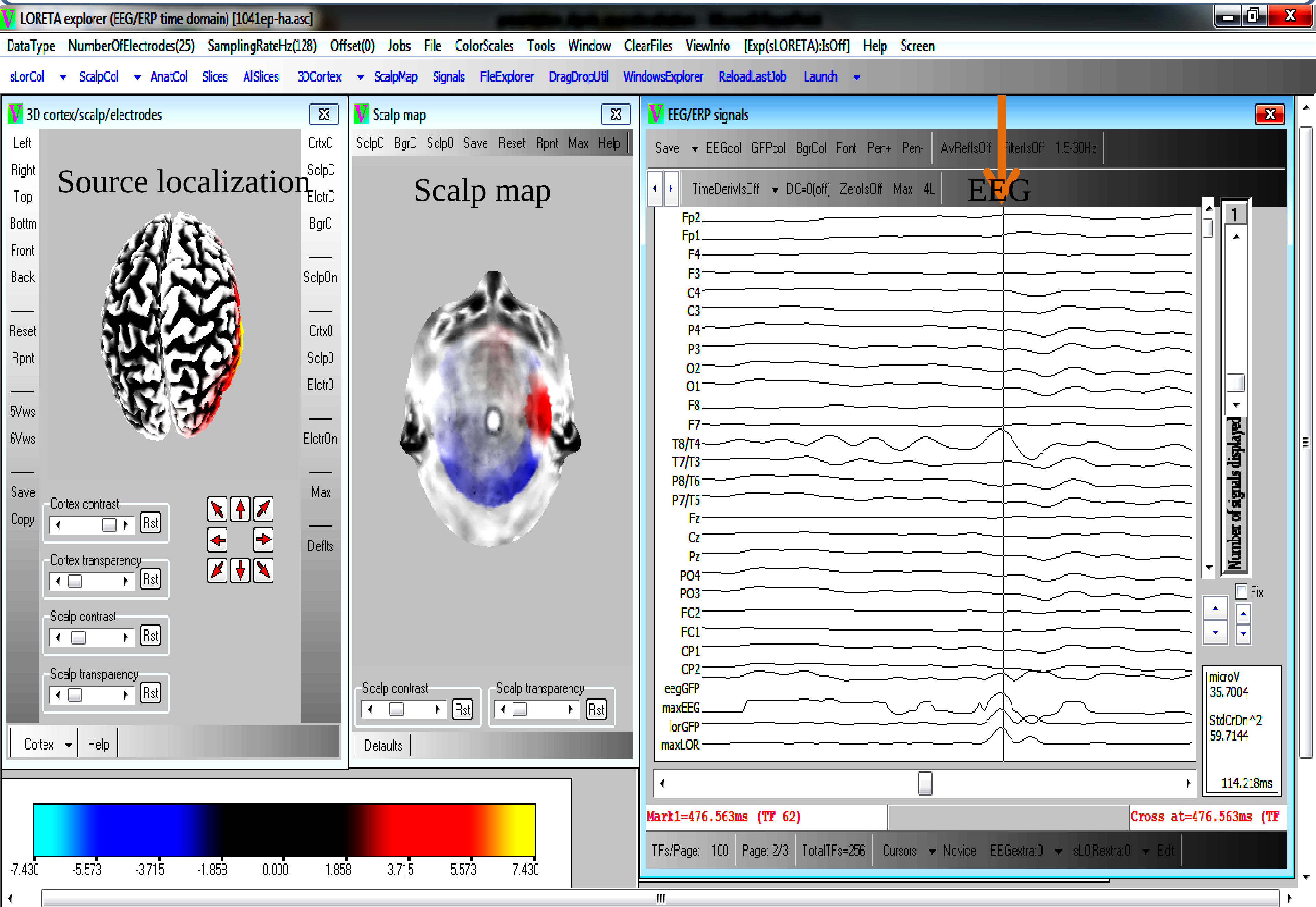

References

1. Wendel K, Väisänen O, Malmivuo J, Gencer NG, Vanrumste B, Durka P, Magjarevic R, Supek S, Pascu ML, Fontenelle H, de Peralta Menendez RG. EEG/MEG source imaging: methods, challenges, and open issues. Computational intelligence and neuroscience. 2009 Jan 1;2009:13.
2. Hallez H, Vanrumste B, Grech R, Muscat J, De Clercq W, Vergult A, D'Asseler Y, Camilleri KP, Fabri SG, Van Huffel S, Lemahieu I. Review on solving the forward problem in EEG source analysis. Journal of neuroengineering and rehabilitation. 2007 Dec;4(1):46.
3. Grech R, Cassar T, Muscat J, Camilleri KP, Fabri SG, Zervakis M, Xanthopoulos P, Sakkalis V, Vanrumste B. Review on solving the inverse problem in EEG source analysis. Journal of neuroengineering and rehabilitation. 2008 Dec;5(1):25.
4. http://www.uzh.ch/keyinst/loreta
5. He Y, Liang B, Yang J, Li S, He J. An iterative closest points algorithm for registration of 3D laser scanner point clouds with geometric features. Sensors. 2017 Aug 11;17(8):1862.
6. D. J. Kroon, "Iterative Closest Point using finite difference optimization to register 3D point clouds affine," http://www.mathworks.com/matlabcentral/fileexchange/24301-finite-iterative- closest-point.
7. Ashburner J, Friston KJ. Unified segmentation. Neuroimage. 2005 Jul 1;26(3):839-51.
8. Sazonov I, Nithiarasu P. Semi-automatic surface and volume mesh generation for subject-specific biomedical geometries. International Journal for Numerical Methods in Biomedical Engineering. 2012 Jan 1;28(1):133-57.
9. de Peralta-Menendez RG, Gonzalez-Andino SL. Comparison of algorithms for the localization of focal sources: evaluation with simulated data and analysis of experimental data. International Journal of Bioelectromagnetism. 2002; 4(1).
10. Staljanssens W, Strobbe G, Van Holen R, Keereman V, Gadeyne S, Carrette E, Meurs A, Pittau F, Momjian S, Seeck M, Boon P. EEG source connectivity to localize the seizure onset zone in patients with drug resistant epilepsy. NeuroImage: Clinical. 2017 Jan 1;16:689-98.